STUDY OF PdNi BIMETALLIC NANOPARTICLES SUPPORTED ON CARBON BLACK FOR ANION EXCHANGE MEMBRANE FUEL CELLS

Van Men Truong[1], Quang Khoa Dang[2], Ngoc Bich Duong[3], HsiharngYang[4]
[1] *School of Engineering and Technology, Tra Vinh University, Vietnam*
[2] *HCMC University of Technology and Education University, Vietnam*
[3] *School of Agriculture and Aquaculture, Tra Vinh University, Vietnam*
[4] *National Chung Hsing University, Taichung City 402, Taiwan*

Received 17/4/2020, Peer reviewed 20/4/2020, Accepted for publication 15/5/2020.

ABSTRACT

Anion exchange membrane fuel cells (AEMFCs) have recently received significant attention due to their potential to use non-Pt catalysts. In this work, we developed bimetallic PdNi nanoparticles supported on Vulcan XC72R carbon black (PdNi/C) using a wet impregnation method applied to AEMFC anode electrodes. The PdNi/C electrocatalysts containing a similar metal content (40% by weight) over carbon content (60% by weight) with various Pd:Ni weight % ratios are synthesized and evaluated. The X-ray diffraction patterns confirm the successful preparation of PdNi/C electrocatalyst and the estimated Pd crystallite size is around 2.5 nm. In addition, the X-ray photoelectron spectroscopy also indicates that the coexistence of PdNi bimetallic structure is observed in the catalyst sample. A single H_2/O_2 AEMFC testing using a bimetallic PdNi/C anode catalyst and a commercial Pt/C cathode catalyst shows the highest peak power density of about 302 mW cm^{-2} for the Pd:Ni wt.% ratio of 50:50, which is consistent with cyclic voltammetry measurements. This result indicates that the PdNi/C catalyst has a high potential for using in AEMFCs.

Keywords: *Anion Exchange Membrane Fuel Cell; PdNi/C catalyst; Non-PGM catalyst; anode catalyst; Fuel cell performance.*

1. INTRODUCTION

Fuel cell technology has long been considered as an alternative energy source to the progressive concern with the fast declination and negative environmental impact of fossil fuels. Recently, anion exchange membrane fuel cells (AEMFCs) have attracted interest from researchers as a lower-cost alternative to proton exchange membrane fuel cells (PEMFCs) [1]. One of the merits of AEMFCs is the possibility of using less expensive electrocatalysts and low-cost metal hardware due to the basic environment existing in AEMFCs [2]. Basically, the AEMFC operating principle is similar but not identical to that of PEMFCs. However, their different conduction media (acid in PEMFCs and alkaline in AEMFCs) between the anode and cathode result in the different formation of products. As compared with the PEMFCs in which water is only produced at the cathode, AEMFCs simultaneously involve in the production and consumption of water at the anode and cathode, respectively. Figure 1 depicts a typical AEMFC schematic diagram based on a sandwich structure composed of an anode electrode, membrane, and cathode electrode. The electrochemical reactions of AEMFCs via OH^- conduction within the anion exchange membrane can be given as follows.

Anode: $2H_2 + 4OH^- \rightarrow 4H_2O + 4e^-$ (1)

Cathode: $O_2 + 2H_2O + 4e^- \rightarrow 4OH^-$ (2)

Overall: $2H_2 + O_2 \rightarrow 2H_2O$ (3)

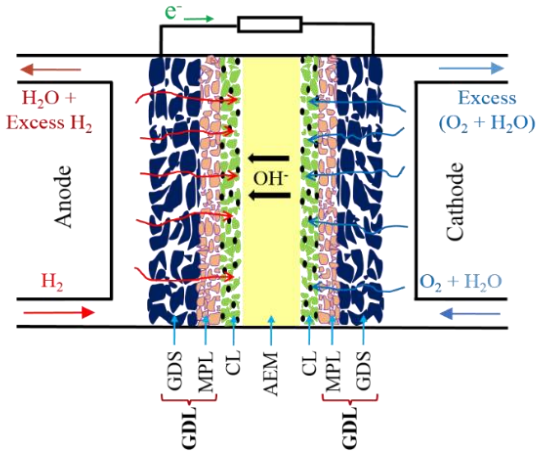

Figure 1. *Schematic diagram of a typical AEMFC [3].*

In the last decade, while numerous attempts have been put on the development of oxygen reduction reaction (ORR) catalysts in alkaline medium [4], research on hydrogen oxidation reaction (HOR) catalysts for AMFCs constitute a practically new field of investigation because of the sluggish of the HOR kinetics in alkaline media compared to acid media [5], even though it is for the case of using platinum (Pt). In the search for platinum-free catalyst candidates for HOR in alkaline media, palladium showed a good selection since a Pd face-centered cubic (fcc) structure has the same significant properties of atomic size and electronic configuration as those of Pt and it is reasonably priced and enormously abundant in comparison to Pt. However, although it was reported that Pd followed the same trend as Pt, Pd/C exhibits 20 times lower exchange current density than Pt/C in alkaline medium [6]. Therefore, Pd-based binary catalysts have been considered as a good direction to study. For instance, Yin et al. [7] prepared bimetallic PdAg nanoparticles supported on carbon black through the emulsion-assisted ethylene glycol ternary system for methanol oxidation in alkaline media. They concluded that carbon-supported $Pd_{80}Ag_{20}$ nanoparticles exhibited a distinctly superior activity for the methanol oxidation, even if compared with commercial Pt/C electro-catalyst. Alia et al. [8] also reported that Pd coated Cu nanowires can produce specific activities towards HOR in rotating disk electrode half-cells 20 times greater than Pd nanoparticles and close to Pt/C in a basic environment. In addition, Qi et al. [9] found that the PdAg/CNT showed a high activity towards alcohol oxidation reaction (alcohol = methanol, ethanol, ethylene glycol, and glycerol)anion exchange membrane direct alcohol fuel cells (AEM-DAFCs) owing to several reasons such as: (i) Ag can help Pd to accelerate the reaction rate of aldehyde oxidation reaction; (ii) A high value of the electrochemically active surface area of PdAg/CNT can be achieved due to a reduction of Ag particle size through alloying with Pd; (iii) PdAg/CNT can improve high fuel efficiency by cleaving the C-C bond of long-chain polyols. Similarly, Lim et al. [10] examined the electrochemical activity of Pd-based binary catalysts (PdM, M = Ru, Sn, or Ir) supported on reduced graphene oxide (RGO) for electro-oxidation of methanol, ethanol, or 1-propanol, in alkaline media. Their results showed that the Pd-based binary systems could significantly improve electrocatalytic performance compared to the monometallic Pd/RGO catalyst.

In addition, the combination of Pd and Ni in which Pd nanoparticles is covered on the Ni nanoparticles, denoted as $Pd_{shell}Ni_{core}$, has been investigated by several researchers. Specifically, Chen et al. [11] prepared $Pd_{shell}Ni_{core}$ catalyst decorated carboxylated multi-walled carbon nanotubes (PdNi/CNT) using a two-stage polyol method for alkaline glucose electrooxidation. The electrochemical surface area and current density of the PdNi/CNT catalyst had 4.5 and 1.5 times higher than those of the Pd/CNT catalyst, respectively. By using the rotating disc electrode technique, Bakos [12] confirmed that the PdNi bimetallic catalyst can provide a better exchange current during HOR in alkaline solution (10 times higher than pure Pd). A low Pd coverage (~17%) is sufficient to reach a diffusion limit for the HOR process. Shviro [13] also demonstrated that using organometallic precursors instead of using metalorganic precursors to

synthesize Ni@Pd core–shell nanoparticles have much higher specific activity towards HOR in 0.1M KOH solution. In addition, a better HOR activity of the Ni@Pd core–shell nanoparticles can be due to a bifunctional electrocatalytic mechanism with hydrogen binding on Pd and OH binding on Ni. In a previous work, Alesker et al. reported for the first time that a mixture of Ni and Pd nanoparticles exhibit a favourable metal–metal interaction that enhances the AEMFC anode HOR reactivity as compared with an anode using the same loading of Pd alone [14].

From the recent literature, it can be seen that Pd-based binary catalysts, especially, PdNi nanoparticles, exhibited a good catalytic activity for HOR in alkaline media and it is a possible alternative over Pt-based catalysts in AEMFCs. However, to our knowledge, the PdNi/C is limited to evaluating in a real AEMFC. Therefore, in this work, we develop PdNi bimetallic nanoparticles supported on carbon black (Vulcan XC72R), namely PdNi/C, using a wet impregnation method applied to the AEMFC anode electrode. The PdNi/C electrocatalysts are prepared by keeping the same metal (PdNi) and carbon (C) content (40% and 60% by weight, respectively) while varying the wt.% ratio of Pd to Ni. The as-prepared PdNi/C are characterized using X-ray diffraction (XRD), X-ray photoelectron spectroscopy (XPS), and cyclic voltammetry (CV). Finally, the performance of a single H_2/O_2 AEMFC using the PdNi/C and commercial Pt/C as anode and cathode catalysts, respectively, is carefully evaluated.

2. EXPERIMENTS

2.1 Materials

Palladium chloride ($PdCl_2$), Nickel (II) chloride hexahydrate ($NiCl_2{\cdot}6H_2O$), Sodium hydroxide (NaOH), Isopropyl alcohol (IPA), and Potassium hydroxide(KOH)were purchased from Sigma-Aldrich and used as received without any further purification. Carbon Vulcan XC-72R was obtained from Cabot Corporation. 40% Pt/C was purchased from Tanaka Holdings Co., Ltd., Japan while anion exchange membrane aQAPS-S_8 and ionomer aQAPS-S_{14} obtained from Hephas Energy Co., Ltd. Carbon fiber paper (GDL 340+30%PTFE) supplied by CeTech Co Ltd., Taiwan was employed as a gas diffusion layer (GDL). The aQAPS-S_8 membrane with a thickness of 30 – 40 μm in the dry form has an ion exchange capacity (IEC) of ca. 1.0 meq g^{-1} and specific ion conductivity of ca. 0.1 S cm^{-1} at 60 ^oC. The utilization of aQAPS-S_{14} ionomer along with aQAPS-S_{14} membrane is beneficial for better performance (as suggested by the supplier). Deionized (DI) water (18.2 MΩcm) was used to prepare all aqueous solutions.

2.2 Synthesis of the PdNi/C catalyst

In this work, to prepare PdNi/C catalyst, Palladium chloride ($PdCl_2$) and Nickel (II) chloride hexahydrate ($NiCl_2{\cdot}6H_2O$) were used as precursors while sodium borohydride ($NaBH_4$) was used as (a) reducing agent. In a typical preparation of 50:50PdNi/C, 200 mg of Vulcan XC-72R was dispersed in 136mL DI water by sonication for 30 min and then, by magnetic stirring for 6 h before adding 63 mL 0.01 M $PdCl_2$ and 113.6 mL 0.01 M $NiCl_2{\cdot}6H_2O$ solutions. The pH of the mixture was adjusted to above pH 10 using the 0.1 M NaOH solution. After that, 150 mL $NaBH_4$ solution with a concentration of 2 mg/mL $NaBH_4$ was slowly added and vigorously stirred with a rotating shaker for 12 h at room temperature (~25 ^oC). The suspension was then filtered and washed with DI water for 5 times. Finally, the collected particles were dried in an oven for 8 h at 80 °C. The different wt.% ratios of Pd to Ni were obtained by determining the weight of Pd and Ni during the synthesis process. The wt.% ratio of PdNi to C which is 40:60 is kept the same for all experiments.

2.3 PdNi/C catalyst characterization

The chemical composition, crystallographic structure, and particle size of the as-synthesized catalyst materials were characterized using high-resolution X-ray

diffractometer (HRXRD, BRUKER D8 SSS) and X-ray photoelectron spectroscopy (XPS). For electrochemical characterization, cyclic voltammetry (CV) measurements were conducted by using a three-electrode configuration connected to a potentiostat (600E workstation, CH Instruments, Inc.). In particular, a glassy carbon electrode (GCE) with a geometric area of 0.071 cm^2, an Ag/AgCl (0.196 V vs. SHE), and a Pt wire were used as the working electrode, reference electrode, and counter electrode, respectively. Before each test, the GCE working surface was polished with 0.05 µm alumina slurry on a polishing pad for 5 min, followed by rinsing with deionized (DI) water in an ultrasonic bath for 15 min. The catalyst ink was prepared by mixing the catalyst with DI water, isopropyl alcohol (IPA) and aQAPS-S_{14} ionomer. All electrodes were immersed in 1 M KOH solution prepared from KOH pellets and the experiments were performed at room temperature.

2.4 Membrane electrode assembly and fuel cell test

The catalyst performance was evaluated using a single AEMFC. The synthesized catalysts were incorporated in the membrane electrode assembly (MEA) as the anode catalyst along with a commercially available Pt/C (40% Pt, Tanaka Holdings Co., Ltd., Japan) as the cathode catalyst. The catalyst layers were prepared as follows: the catalyst ink was prepared by adding the determined amount of the catalysts (PdNi/C and Pt/C for anode and cathode electrodes, respectively) to 400 mg DI water. Then, 20 wt.% of the aQAPS-S_{14} ionomer and 400 mg of IPA was added to the mixture and sonicated for more than 40 min to obtain homogeneity. The resulting catalyst ink was coated onto the microporous layer (MPL) of the gas diffusion layer by hand-brushing on a hot plate of 80 ^oC to form gas diffusion electrodes (GDEs). The catalyst loadings were 1.5 mg_{PdNi} cm^{-2} and 0.8 mg_{Pt} cm^{-2}. Since the aQAPS-S8 membrane and aQAPS-S14 ionomer were originally in chloride form (Cl-), pre-treatment for the membrane and prepared GDEs was performed to convert Cl- into the hydroxide form (OH-) by soaking in 1 M KOH for 48 h.

Finally, the aQAPS-S_8 membrane was sandwiched between the two electrodes without hot pressing. The active electrode area was 10.24 cm^2. Two Teflon gaskets of 250 µm thickness located between graphite plates with machined triple serpentine flow channels (1 mm channel width, 1 mm channel height, and 1.5 mm rib width) and gas diffusion electrodes were used to provide a 20–30% GDL compression. Two gold-coated copper plates were employed as current collectors. The fixture was then sealed using 8 bolts with a constant torque of 1.47 Nm. This cell fixture was attached to the fuel cell test station (FCED-PD50) for the polarization measurements.

3. RESULTS AND DISCUSSION

3.1 Morphological and structural of PdNi/C composites

The bulk structural information of the PdNi/C was obtained by XRD as presented in Fig.2. The broad peak at around 2θ value of about 25° can be assigned to carbon (002) facet [15]. All XRD data confirm the presence of Pd and Ni particles in the PdNi/C sample. In particular, the recorded XRD patterns of the PdNi/C catalyst shows that there are four main diffraction peaks with 2θ values of around 40.1°, 46.2°, 67.5°, and 82.1° which can be assigned to the (111), (200), (220), and(311) facets of the face-centered cubic (fcc) crystal structure of Pd, respectively [10, 16].On the other hand, the small diffraction peaks at 2θ values of about 33.3° and 59.4° can be attributed to $Ni(OH)_2$ (100) and (110) facets, respectively [17]. It is noted that the diffraction peaks of the $Ni(OH)_2$ (100) and (110) facets observed instead of pure Ni could be due to the measured samples were not completely dried. Moreover, a higher Pd content results in a stronger crystalline phase, whereas the samples with the lower Pd contents are in more amorphous states, and the peak intensity of the Pd (200), Pd (220) and Pd

(311) facets are not clear. Similarly, as the Ni content is less, the peak intensities of $Ni(OH)_2$(100) and (110) facets are not obvious probably due to the poor crystallization properties of Ni particles. Besides, as the Pd content increases, the PdNi diffraction peaks show a slight shift toward higher 2θ values, indicating that a better PdNi bimetallic alloy structure is formed. The Pd (111) peak was employed to estimate the average crystallite size from Scherrer's equation [18]:

$$d = \frac{0.9 \times \lambda}{B_{2\theta} \times \cos\theta} \quad (4)$$

where d is the crystallite size, λ is the wavelength of X-ray radiation (here is 0.15406 nm), $B_{2\theta}$ is the peak width at the half-maximum intensity, and θ is the Bragg angle (the diffraction angle of the maximum peak (111)). According to this equation, the average size of the Pd particles was estimated to be around 2.5 nm in the PdNi/C catalysts. This result is similar to the report in [19].

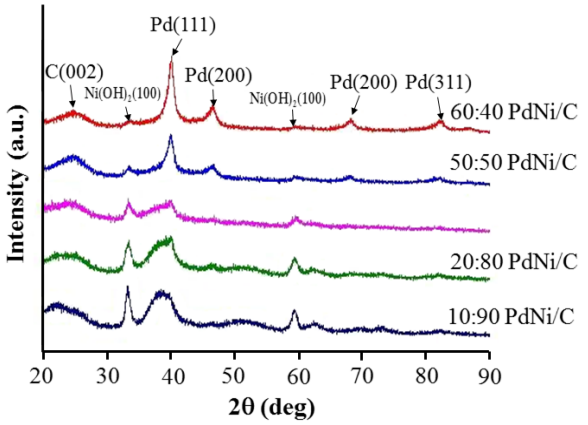

Figure 2. *XRD patterns of the PdNi/C catalysts with various wt.% ratios of Pd to Ni.*

The surface composition of 50:50 PdNi/C was further confirmed using X-ray photoelectron spectroscopy (XPS) as shown in Fig. 3. The chemical compositions of the catalyst can be analyzed by deconvolution of the original spectra. The XPS peaks of Ni (2p), O (1s), Pd (3d), and C (1s) are observed in the XPS spectra. In addition, Fig. 4(a) shows the characteristic spin-orbit doublets for the palladium system with two binding energy peaks located at 335.7 and 341 eV correlated to Pd $3d_{5/2}$ and Pd $3d_{3/2}$, respectively, and ascribed to metallic Pd. The other located at 335.7 eV is contributions from the adsorbed oxygen-palladium interaction (PdO_{ads}) and PdO species. Comparing to the standard Pd0 3d5/2 located at 335.0 eV, it reveals that the as-prepared catalysts shift to higher Pd core levels. It is known that a positive core-level shift of Pd can be interpreted as an electron loss of the Pd atoms, which will lead to a lower d-band center of Pd. Accordingly, the results indicate that there is an existence of an electron interaction between Pd and Ni. Similarly, Fig. 4(b) shows the characteristic spin-orbit coupling for the Ni system with two binding energy peaks at 855.8eV and 874.1eV which can be assigned to Ni $2p_{3/2}$ and Ni $2p_{1/2}$ [20]. The peaks located at 861 and 880 eV are shake-up peaks arising from multi-electron excitation. Moreover, deconvolution of the Ni 2p peaks revealed that the nickel species present are in the oxidized states, at 855 eV from $Ni(OH)_2$. The existence of $Ni(OH)_2$ may stem from the possibility that the surface-bound nickel atoms are prone to react with atmospheric O_2 and H_2O to form the oxide species due to the oxophilic nature of the Ni metal. Thus, these results further demonstrate the successful synthesis of PdNi alloy on the carbon particles.

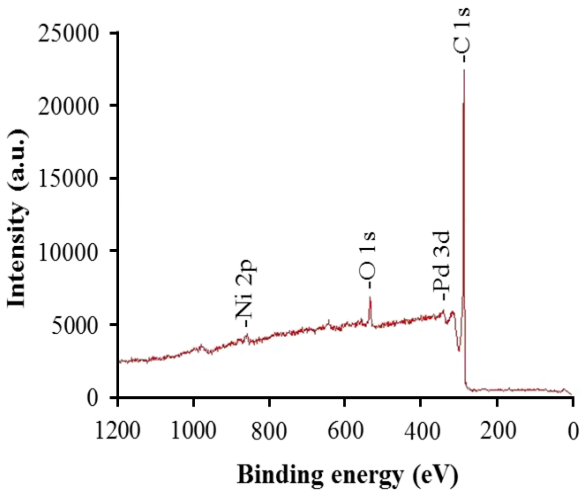

Figure 3. *The wide survey XPS spectra of 50:50 PdNi/C*

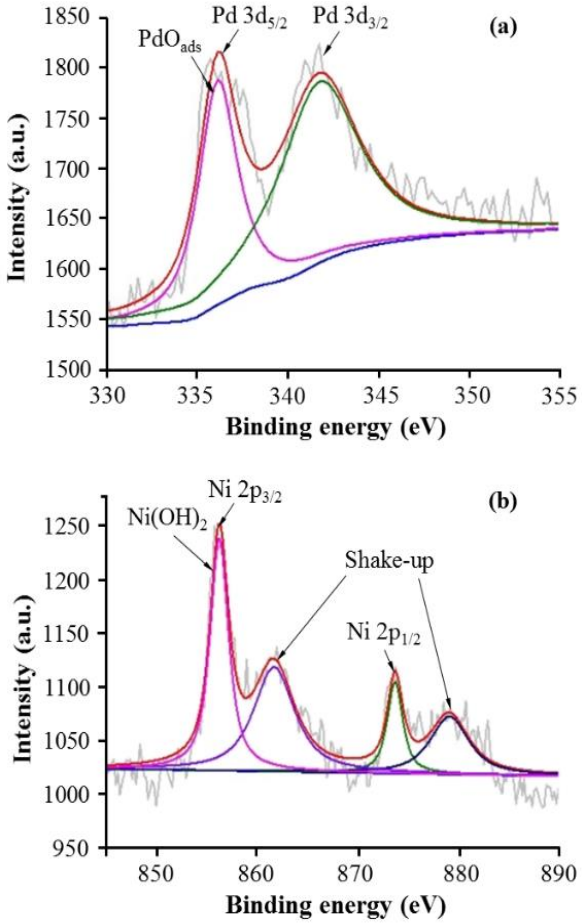

Figure 4. *The survey XPS spectra of the 50:50 PdNi/C for: (a)Pd 3d and (b) Ni 2p*

3.2 Electrochemical characterization of the electrocatalysts

The electrochemical characterizations of the synthesized PdNi/C were investigated by CV measurements. Fig. 5 shows the measured CV patterns of the PdNi/C catalysts in 0.1 M KOH solution with the scan rate of 20 mV s^{-1}. The purpose of this experiment is to evaluate the electrochemical active surface area (EASA) for different Pd and Ni weight ratios. From the CV results, we can see that, in all cases, the palladium reduction/oxidation and hydrogen absorption/desorption regions are observed. The peaks of the hydrogen adsorption/desorption on the PdNi surface appeared at around 0.2 to 0.4 V vs. RHE in the forward scan. In addition, the corresponding peaks ranging from *ca.* 0.55 to 0.8 V vs. RHE in the back scan is ascribed to the Pd oxide reduction.

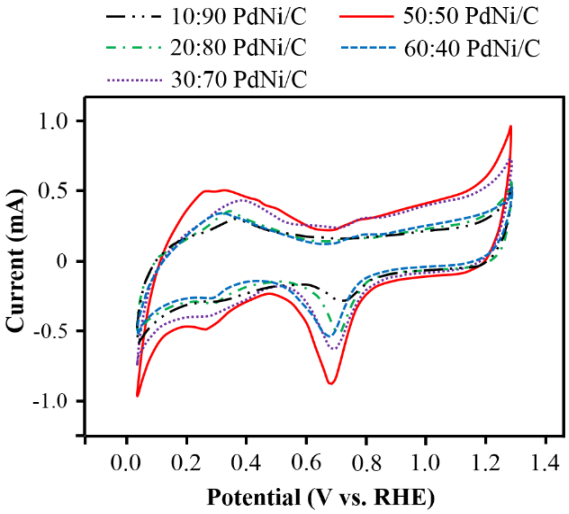

Figure 5. *CV curves of the PdNi/C catalysts with various Pd to Ni wt.% ratios, in 1 M KOH solution with a scan rate of 20 mV s^{-1}.*

For the sake of hydrogen dissolving into the Pd bulk, the electrochemically active surface area (EASA) cannot be estimated using the adsorption/desorption peaks of hydrogen. According to the charge of the palladium oxide reduction peaks, the ECSA of the Pd-based alloys can be calculated by the following Eq. [13, 21, 22].

$$EASA = \frac{Q_S}{Q_C \times m} \times 10^{-4} \quad (5)$$

where Q_S is the coulomb charge (in μC) determined by integrating the current peak of PdO reduction, Q_C is the conversion factor and has been commonly taken as 420 μCcm^{-2} corresponding to PdO reduction, and m is the loadings of Pd catalyst (in g) on the GC surface. Based upon the methods mentioned above, the EASA values of the PdNi/C catalysts were evaluated and are listed in Table 1. These distinct measurements show that the EASA of the PdNi/C catalysts increases with increasing the Pd wt.% and the largest estimated EASA is obtained for the 50:50 PdNi/C catalyst (~20.6 m^2 g^{-1}). This is because that increasing Pd metal content means more Pd particles present in the PdNi/C catalyst, resulting in a higher EASA. However, an over Pd content (60 wt.%) causes a decrease in the EASA. It could be due to that

removing Ni particles while adding more Pd particles (as increasing Pd wt.% and decreasing Ni wt.%) will lead to a lack of Ni surface for the PdNi bimetallic formation and thereby reducing the EASA of the catalyst. In general, the results indicate that there is a balance between Pd and Ni contents as preparing PdNi/C catalysts for obtaining the highest EASA.

Table 1. *Parameters involved in the EASA estimation of the PdNi/C catalyst using PdO reduction*

Pd:Ni	Metal loading (mg)	Integral coulomb (μC)	EASA (m^2g^{-1})
60:40	0.1	5830	13.7
50:50	0.1	8740	20.6
30:70	0.1	6285	14.8
20:80	0.1	4400	10.4
10:90	0.1	2500	9.5

3.3 Single AEMFC cell performance

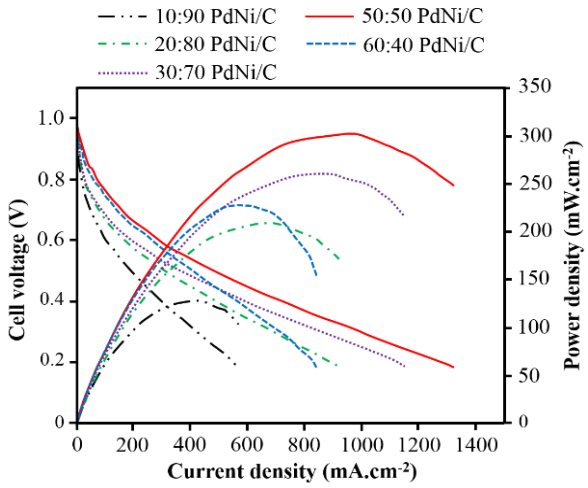

Figure 6. *Polarization and power density curves using the PdNi/C as anode catalyst.*

The polarization and power density curves of a single H_2/O_2AEMFC using the as-prepared PdNi/C as the anode catalyst are presented in Fig.6. Such a single cell was operated at a cell temperature of 70°C and controlled dew points of 68°C and 73°C for H_2 and O_2, respectively. The testing results show that the single cell performance significantly increases with increasing the Pd loading from 10 to 50 wt.% in the synthesized PdNi/C catalysts. In particular, the peak power densities of the single cell are 127, 209, and 260 $mWcm^{-2}$ for integrating the 10:90 PdNi/C, 20:80 PdNi/C, 30:70 PdNi/C catalysts as anode catalysts, respectively and reaches the highest value of 302 $mWcm^{-2}$ with the 50:50 PdNi/C catalyst. However, there is a considerable decrease in the peak power density (227 $mWcm^{-2}$) for the case of using the 60:40 PdNi/C catalyst. One of the main reasons for the variation of the cell performance with using PdNi/C catalysts having different ratios of Pd to Ni is the difference in EASA. The best performance of the 50:50 PdNi/C catalyst in comparison to the other cases can be ascribed to the higher EASA which is in good agreement with the measured CV trend. Besides, it is also noted that although it is not really reasonable to compare the results observed in this work to those reported in the recent literature due to their distinct experiments, the achieved cell performance reveals that the PdNi/C catalyst exhibits a high potential to use in AEMFCs in terms of Pt replacement.

4. CONCLUSIONS

PdNi/C bimetallic electrocatalysts have been synthesized by a wet impregnation method and tested with a single AEMFC. The physicochemical characterization of the catalysts confirms that the PdNi bimetallic nanostructure is successfully attached onto the carbon support and there is an ideal ratio of Pd to Ni which can produce the highest EASA. For the single AEMFC testing, the results show that the highest peak power density is achieved with the 50:50 PdNi/C which is in good agreement with the estimated EASA obtained from CV measurements. These results along with previous studies further reveal that PdNi bimetallic catalyst shows great potential for HOR in alkaline media, especially in AEMFCs. Further our investigation of the mechanism for HOR on the PdNi surface and the catalytic durability in alkaline media is under construction.

ACKNOWLEDGEMENTS

We are grateful to Professor Hsiharng Yang for his guidance and financial support. Authors are thankful to CeTech Co Ltd., Taiwan for supplying GDL materials.

REFERENCES

[1] Z. Yang, J. Ran, B. Wu, L. Wu, T. Xu, (2016). Stability challenge in anion exchange membrane for fuel cells. *Current Opinion in Chemical Engineering*, 12, 22-30.

[2] J. Varcoe, P. Atanassov, D. Dekel, A. Herring, M. Hickner, P. Kohl, A. Kucernak, W. Mustain, K. Nijmeijer, K. Scott, T. Xu, L. Zhuang, (2014). Anion-exchange membranes in electrochemical energy systems. *Energy Environ. Sci.*, 7, 3135.

[3] V. M. Truong, M.-K. Yang, H. Yang, (2019). Functionalized Carbon Black Supported Silver (Ag/C) Catalysts in Cathode Electrode for Alkaline Anion Exchange Membrane Fuel Cells. *International Journal of Precision Engineering and Manufacturing-Green Technology*, 6(5), 711-721.

[4] J. S. Spendelow, A. Wieckowski, (2007). Electrocatalysis of oxygen reduction and small alcohol oxidation in alkaline media. *Phys. Chem. Chem. Phys.*, 9(21), 2654-2675.

[5] K. C. Neyerlin, W. Gu, J. Jorne, H. A. Gasteigera, (2007). Study of the Exchange Current Density for the Hydrogen Oxidation and Evolution Reactions. *Journal of The Electrochemical Society*, 154(7), B631-B635.

[6] J. Durst, A. Siebel, C. Simon, F. Hasché, J. Herranz, H. A. Gasteiger, (2014). New insights into the electrochemical hydrogen oxidation and evolution reaction mechanism. *Energy Environ. Sci.*, 7(7), 2255-2260.

[7] Z. Yin, Y. Zhang, K. Chen, L. Jing, W. Li, P. Tang, H. Zhao, Q. Zhu, X. Bao, D. Ma, (2014). Monodispersed bimetallic PdAg nanoparticles with twinned structures: Formation and enhancement for the methanol oxidation. *Scientific reports*, 4, 4288.

[8] S. M. Alia, Y. Yan, (2015). Palladium Coated Copper Nanowires as a Hydrogen Oxidation Electrocatalyst in Base. *J Electrochem Soc*, 162(8), F849-F853.

[9] J. Qi, N. Benipal, C. Liang, W. Li, (2016). PdAg/CNT catalyzed alcohol oxidation reaction for high-performance anion exchange membrane direct alcohol fuel cell (alcohol=methanol, ethanol, ethylene glycol and glycerol). *Applied Catalysis B: Environmental*, 199, 494-503.

[10] E. J. Lim, Y. Kim, S. M. Choi, S. Lee, Y. Noh, W. B. Kim, (2015). Binary PdM catalysts (M = Ru, Sn, or Ir) over a reduced graphene oxide support for electro-oxidation of primary alcohols (methanol, ethanol, 1-propanol) under alkaline conditions. *Journal of Materials Chemistry A*, 3(10), 5491-5500.

[11] C. C. Chen, L. C. Chen, (2015). Synthesis and characterization of Pd–Ni core–shell nanocatalysts for alkaline glucose electrooxidation. *RSC Advances*, 5(66), 53333-53339.

[12] I. Bakos, A. Paszternák, D. Zitoun, (2015). Pd/Ni Synergestic Activity for Hydrogen Oxidation Reaction in Alkaline Conditions. *Electrochimica Acta*, 176, 1074-1082.

[13] K. Mohanraju, L. Cindrella, (2014). Impact of alloying and lattice strain on ORR activity of Pt and Pd based ternary alloys with Fe and Co for proton exchange membrane fuel cell applications. *RSC Advances*, 4(23), 11939-11947.

[14] M. Alesker, M. Page, M. Shviro, Y. Paska, G. Gershinsky, D. R. Dekel, D. Zitoun, (2016). Palladium/nickel bifunctional electrocatalyst for hydrogen oxidation reaction in alkaline membrane fuel cell. *Journal of Power Sources*, 304, 332-339.

[15] V. M. Truong, M. K. Yang, H. Yang, (2019). Functionalized Carbon Black Supported Silver (Ag/C) Catalysts in Cathode Electrode for Alkaline Anion Exchange Membrane Fuel Cells. *International Journal of Precision Engineering and Manufacturing-Green Technology*, 6(4), 711-721.

[16] Z. Yan, Z. Hu, C. Chen, H. Meng, P. K. Shen, H. Ji, Y. Meng, (2010). Hollow carbon hemispheres supported palladium electrocatalyst at improved performance for alcohol oxidation. *Journal of Power Sources*, 195(21), 7146-7151.
[17] M. Wang, W. Liu, C. Huang, (2009). Investigation of PdNiO/C catalyst for methanol electrooxidation. *Int J Hydrogen Energy*, 34(6), 2758-2764.
[18] L. L. He, P. Song, J. J. Feng, W. H. Huang, Q. L. Wang, A. J. Wang, (2015). Simple wet-chemical synthesis of alloyed PdAu nanochain networks with improved electrocatalytic properties. *Electrochimica Acta*, 176, 86-95.
[19] D. Łomot, Z. Karpiński, (2016). Catalytic activity of Pd-Ni in the oxidation of hydrogen for the safety of nuclear power plant. *Polish Journal of Chemical Technology*, 18.
[20] B. Payne, M. Biesinger, N. McIntyre, (2009). The study of polycrystalline nickel metal oxidation by water vapour. *Journal of Electron Spectroscopy and Related Phenomena*, 175, 55-65.
[21] C. Xu, Y. Liu, Q. Hao, H. Duan, (2013). Nanoporous PdNi alloys as highly active and methanol-tolerant electrocatalysts towards oxygen reduction reaction. *Journal of Materials Chemistry A*, 1(43), 13542-13548.
[22] W. Pan, X. Zhang, H. Ma, J. Zhang, (2008). Electrochemical Synthesis, Voltammetric Behavior, and Electrocatalytic Activity of Pd Nanoparticles. *J Phys Chem C*, 112(7), 2456-2461.

Corresponding author:
Truong Van Men
School of Engineering and Technology, Tra Vinh University
Email: tvmen@tvu.edu.vn